78-726

Section Design for Hydrofoil Wings with Flaps

Young T. Shen*
David W. Taylor Naval Ship Research and Development Center, Bethesda, Md.
and
Richard Eppler†
Universität Stuttgart, Germany

The basic problem of a flapped NACA-16 foil is its poor pressure distribution around the flapped region. With the flap deflected, the velocity distribution becomes a very unfavorable shape in terms of cavitation-inception and boundary-layer separation. This type of flowfield results in low flap effectiveness. Based on the present profile design and boundary-layer calculation methods, improved hydrofoil wings with flaps have been developed. The approaches to construct the desired velocity distributions to delay cavitation and boundary-layer separation are discussed. Examples are given for the case that the flap deflection has to compensate the vertical component of the surface wave motion in a seaway.

Introduction

HYDROFOILS which operate in the subcavitating regime require foil configurations having sufficient strength, minimum weight, and maximum lift-to-drag ratio, while, at the same time, extending the critical cavitation speed to as high a value as practical. These same hydrodynamic requirements made the use of NACA-16 series attractive for hydrofoils. Consequently, this series of wing sections has been extensively applied in the existing hydrofoil craft.[1]

Hydrofoil craft are typically designed to operate in both calm water and waves. In a seaway the lifting surfaces of a hydrofoil craft experience significant changes in angle of attack due to orbital motion and craft motion. The seakeeping quality of a hydrofoil craft depends heavily on the availability of lift compensation to negotiate the hostile environment. Many of the existing hydrofoil craft are equipped with flaps as control devices.

The basic problem of a flapped NACA-16 foil is its poor pressure distribution around the flap region. At the design condition, the velocity distribution over the upper surface is more or less constant up to the beginning of the pressure recovery region.[2] A flap deflection down causes a suction peak at the upper surface near the flap hinge. Additionally, the range of lift coefficients without encountering a suction peak at the leading edge is considerably reduced. Hence, the flapped configuration is unfavorable with respect to cavitation-inception. In addition, the adverse pressure gradient behind the suction peak at flap hinge causes earlier separation. Due to this type of flowfield, NACA-16 series wing sections encounter low flap effectiveness. To circumvent this undesirable feature, another wing section of NACA 64A309 is being evaluated at the David W. Taylor Naval Ship Research and Development Center (DTNSRDC).[3]

The well-known NACA wing sections were developed around the year 1940. A few possible areas of improvements have been observed and discussed in Ref. 4. In addition, the basic thickness forms of these NACA sections were theoretically developed without taking into account the flap deflection. The aim of this paper is to show that by means of available methods of profile design and boundary-layer calculation,[5-7] it is possible to design wing sections with improved hydrodynamic characteristics in terms of cavitation-inception and flap effectiveness. The classic assumption used is that cavitation-inception occurs when the local pressure falls to or below the vapor pressure of the flowing fluid. Flap effectiveness is maintained if cavitation and boundary-layer separation are avoided.

The effect of flap deflection on cavitation-inception will be examined first. The mathematical tools to be used in the section design will be discussed briefly. Finally, two approaches to design wing sections, including the consideration of flap deflection, are presented in Tables 1 and 2.

Flap Deflection and Cavitation-Inception

A NACA 16-309 foil shape was tested by Layne.[3] Relatively poor flap effectiveness was measured in the towing tank at the carriage speed of 38.9 knots, corresponding to a Reynolds number (based on the mean chord) of 2.7×10^6. On the other hand, two-dimensional wind-tunnel tests of the same foil section at the compatible Reynolds number show a significant increase in lift even at relatively large flap deflection.‡ This increase indicates that the effect of cavitation on the nature of flow separation may not be small. Additionally, the existence of a free-surface, strut, pod, finite-aspect ratio, and gap at the hinge line may play a role in producing a significant deviation in the two test results. This paper distinguishes between hydrofoils and aircraft wings in terms of cavitation.

Trailing edge flaps are used for longitudinal and roll control. The effect of pressure peak and phase angle on cavitation-inception was studied recently by Shen and Peterson[8] on a hydrofoil under sinusoidal pitch motion. Due to the complexity of transient loads, the quasi-steady approach will be used in this study. The lift induced by the wave vertical velocity is assumed to be balanced by the lift produced by the deflection of the flap. That means the angle of attack induced by the waves is compensated by the change of the zero lift line caused by the flap deflection. To gain some insight of the wing section design with a flap, two NACA sections of 16-309 ($a = 1.0$) and 64A309 ($a = 0.8$) will be used as examples. Each section is fitted with a trailing edge flap of 25% chord.

The pressure distribution of 16-309 section at flap angles (δ_F) of 0 and 2.5 deg are given in Fig. 1. The flap deflection down is designated as positive. A constant lift coefficient $C_L = 0.22$ is maintained by varying the incidence and flap angles. Even at such a moderate flap angle $\delta_F = 2.5$ deg, the

Presented as Paper 78-726 at the AIAA/SNAME Advanced Marine Vehicles Conference, San Diego, Calif., April 17-19, 1978; submitted May 11, 1978; revision received Oct. 2, 1978.

Index category: Marine Hydrodynamics, Vessel and Control Surface.

*Naval Architect, Ship Performance Department.
†Professor, Institut A für Mechanik.

‡Private communication with the Defence Research Establishment, Atlantic, Canada.

Table 1 Profile 904 coordinates ($\delta_F = 0$ deg)

N	X	Y	N	X	Y	N	X	Y
0	100.000	0.000	37	23.944	5.009	74	27.841	−3.026
1	99.886	.012	38	21.610	4.814	75	30.491	−3.076
2	99.552	.063	39	19.367	4.600	76	33.207	−3.116
3	99.021	.165	40	17.222	4.366	77	35.979	−3.146
4	98.314	.318	41	15.182	4.112	78	38.798	−3.165
5	97.452	.512	42	13.249	3.837	79	41.653	−3.173
6	96.443	.731	43	11.425	3.546	80	44.534	−3.170
7	95.287	.959	44	9.719	3.243	81	47.431	−3.156
8	93.975	1.195	45	8.134	2.930	82	50.335	−3.131
9	92.508	1.445	46	6.677	2.611	83	53.234	−3.095
10	90.895	1.715	47	5.352	2.287	84	56.119	−3.048
11	89.147	2.004	48	4.163	1.962	85	58.979	−2.989
12	87.272	2.312	49	3.115	1.638	86	61.805	−2.918
13	85.283	2.637	50	2.211	1.320	87	64.586	−2.834
14	83.192	2.978	51	1.454	1.011	88	67.313	−2.738
15	81.010	3.329	52	.849	.716	89	69.975	−2.628
16	78.750	3.687	53	.399	.440	90	72.563	−2.503
17	76.427	4.042	54	.108	.192	91	75.068	−2.361
18	74.054	4.386	55	.000	.000	92	77.480	−2.197
19	71.644	4.694	56	.107	−.180	93	79.797	−1.998
20	69.176	4.944	57	.413	−.398	94	82.036	−1.761
21	66.635	5.151	58	.882	−.631	95	84.204	−1.511
22	64.034	5.329	59	1.508	−.870	96	86.287	−1.268
23	61.381	5.477	60	2.287	−1.109	97	88.269	−1.040
24	58.685	5.599	61	3.215	−1.343	98	90.136	−.831
25	55.956	5.694	62	4.287	−1.563	99	91.874	−.647
26	53.202	5.765	63	5.505	−1.761	100	93.469	−.488
27	50.434	5.811	64	6.878	−1.936	101	94.909	−.352
28	47.659	5.832	65	8.403	−2.095	102	96.186	−.234
29	44.888	5.830	66	10.074	−2.242	103	97.297	−.136
30	42.130	5.804	67	11.885	−2.377	104	98.235	−.061
31	39.394	5.756	68	13.828	−2.502	105	98.990	−.015
32	36.690	5.685	69	15.896	−2.615	106	99.545	.004
33	34.025	5.592	70	18.082	−2.718	107	99.885	.004
34	31.409	5.477	71	20.378	−2.811	108	100.000	−.000
35	28.852	5.341	72	22.776	−2.893			
36	26.360	5.185	73	25.266	−2.964			

Table 2 Profile 908 coordinates ($\delta_F = 5.8$ deg)

N	X	Y	N	X	Y	N	X	Y
0	100.000	0.000	37	26.625	5.883	74	24.953	−2.311
1	99.889	.025	38	24.223	5.629	75	27.532	−2.300
2	99.567	.112	39	21.897	5.357	76	30.190	−2.278
3	99.060	.273	40	19.653	5.067	77	32.916	−2.247
4	98.395	.501	41	17.500	4.762	78	35.700	−2.206
5	97.592	.781	42	15.442	4.444	79	38.533	−2.154
6	96.658	1.092	43	13.488	4.114	80	41.403	−2.093
7	95.592	1.418	44	11.642	3.776	81	44.299	−2.020
8	94.381	1.755	45	9.912	3.434	82	47.212	−1.936
9	93.029	2.109	46	8.306	3.089	83	50.130	−1.838
10	91.546	2.484	47	6.829	2.743	84	53.041	−1.724
11	89.942	2.874	48	5.485	2.396	85	55.934	−1.588
12	88.227	3.278	49	4.279	2.052	86	58.810	−1.414
13	86.412	3.688	50	3.214	1.713	87	61.683	−1.209
14	84.509	4.097	51	2.295	1.381	88	64.551	−.993
15	82.529	4.488	52	1.524	1.062	89	67.398	−.780
16	80.464	4.842	53	.905	.758	90	70.209	−.577
17	78.303	5.161	54	.440	.476	91	72.970	−.390
18	76.049	5.455	55	.135	.224	92	75.665	−.223
19	73.710	5.726	56	.002	.023	93	78.281	−.077
20	71.295	5.973	57	.083	−.154	94	80.804	.045
21	68.813	6.198	58	.375	−.355	95	83.219	.142
22	66.271	6.398	59	.832	−.571	96	85.514	.214
23	63.678	6.573	60	1.450	−.793	97	87.676	.263
24	61.044	6.723	61	2.222	−1.014	98	89.693	.289
25	58.376	6.846	62	3.144	−1.230	99	91.555	.295
26	55.684	6.941	63	4.213	−1.437	100	93.251	.284
27	52.977	7.007	64	5.422	−1.630	101	94.771	.260
28	50.264	7.041	65	6.768	−1.803	102	96.110	.229
29	47.554	7.040	66	8.249	−1.944	103	97.265	.193
30	44.849	7.000	67	9.876	−2.051	104	98.229	.151
31	42.152	6.925	68	11.651	−2.133	105	98.993	.104
32	39.473	6.819	69	13.565	−2.197	106	99.549	.056
33	36.819	6.684	70	15.612	−2.246	107	99.887	.017
34	34.199	6.521	71	17.783	−2.280	108	100.000	.000
35	31.622	6.332	72	20.069	−2.302			
36	29.095	6.118	73	22.462	−2.312			

16-series experiences a sharp increase in suction pressure at the hinge line. This causes earlier cavitation at the hinge line, flow separation at the trailing edge, and loss of flap effectiveness. At the neutral flap position, a lift coefficient of $C_L = 0.22$ is produced at the foil angle of $\alpha_x = -0.45$ deg (with respect to the x axis). At a flap angle of $\delta_F = 2.5$ deg, the same lift coefficient is maintained at $\alpha_x = -2.11$ deg. This causes a sharp suction pressure at the lower surface leading edge. Severe leading edge cavitation may be encountered.

The effects of flap deflections on cavitation-inception can be summarized by the minimum pressure envelopes for constant lift coefficients.[9] As examples, these minimum pressure envelopes for constant lift coefficients $C_L = 0.22$ and 0.278, corresponding to craft speeds of 45 and 40 knots at the foil loading of 1250 PSF (60,000 N/m^2) are given in Figs. 2a and 2b. To relate the vapor cavitation number (σ_v) to the craft speeds, the foil is assumed to operate at 1.5 m below the water surface. The total ranges of flap deflection without cavitation ($\Delta\delta_f$) are 5.9 and 6.35 deg at 45 and 40 knots, respectively. The allowable change in angles of attack $\Delta\alpha$ without cavitation are ± 1.75 and ± 1.90 deg for 45 and 40 knots, respectively, if a flap effectiveness ratio of $\Delta\alpha/\delta_f = 0.6$ is used. In the same manner, the allowable change in angles of attack for different lift coefficients can be obtained. Based on the quasi-steady approach, the allowable craft operational envelope is given in Fig. 3. The allowable sea states operable without cavitation can be easily constructed.[9]

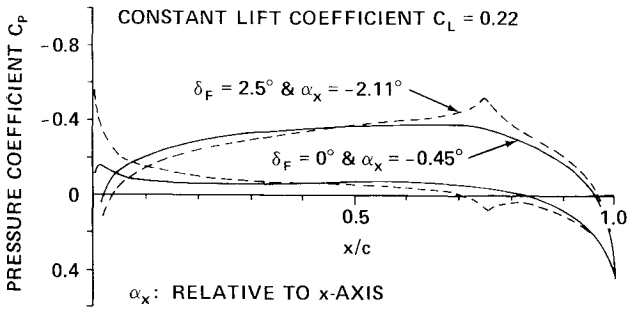

Fig. 1 Pressure distribution of NACA 16-309.

To delay the danger of flow separation and early cavitation at the hinge line, a NACA 64A309 section is currently being evaluated at DTNSRDC. The pressure distributions for $C_L = 0.22$ and flap angles of 0 and 2.5 deg are given in Fig. 4. At the flap angle of 2.5 deg, the suction pressure at the hinge line is lower than it is around $x/c = 0.4$. The relatively low velocity around the flap hinge line provides good flap effectiveness as confirmed in measurements by Layne.[3] However, at the flap angle of $\delta_F = 2.5$ deg, the sharp suction pressure peak at the lower surface leading edge is still present. The minimum pressure envelopes at $C_L = 0.22$ and 0.278 are given in Figs. 2a and 2b, respectively. The allowable craft operational envelope without cavitation is included in Fig. 3.

It is seen that the gain in good flap effectiveness is realized with a significant penalty in $-C_{p\min}$. This is due to the fact that the pressure recoveries begin around 70% chord for the 16-309 sections and 40% chord for the 64A309 sections. The obtainable maximum cruising speed without cavitation differs by almost 5 knots. On the other hand, the relatively low velocity around the flap hinge line on the 64A section provides better flap effectiveness, and allows to tolerate greater fluctuation in angle of attack at speeds lower than 44 knots.

Potential Flow Design and Analysis Theories

The inverse method[5] has been developed to design the coordinates of an airfoil profile from a prescribed velocity distribution $V(\phi,\alpha^*(\phi))$, where ϕ is the polar angle at a circle, into which the profile is conformally mapped. The velocity V is specified sectionally for different angles of attack called $\alpha^*(\phi)$. This α^* is a sectional constant. The ϕ sections may have different sizes. Every section corresponds to a segment of the profile. Except for the pressure recovery area adjacent to the trailing edge, it is adequate to specify $V(\phi,\alpha^*)$ as a constant value. That means the value of α^* in a segment is the significant parameter that specifies the velocity distribution. Should the velocity distribution $V(x, \alpha)$ of the total profile for

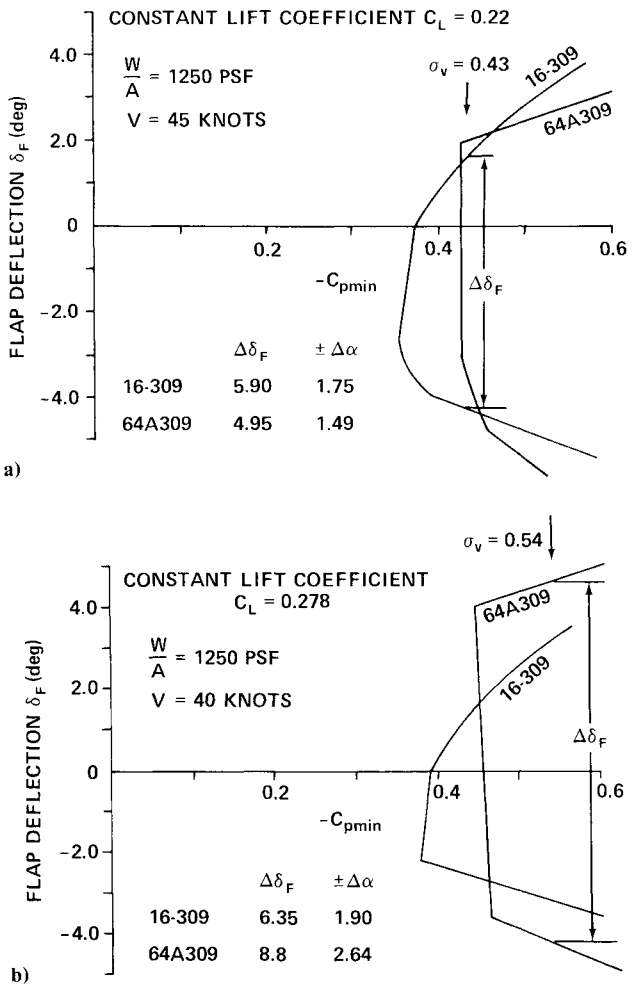

Fig. 2 Minimum pressure envelopes for 16-309 and 64A309.

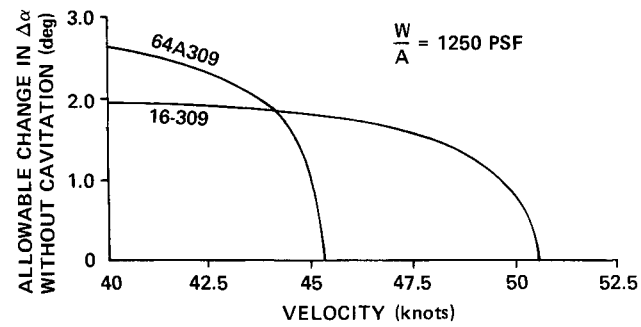

Fig. 3 Allowable change in angles of attack at incipient cavitation speeds for 16-309 and 64A309.

one angle of attack α be considered, then a certain segment of the profile outside of the recovery area $V(x, \alpha) = \text{const}$, if $\alpha = \alpha^*$. For a given α, the pressure gradient in a segment can be influenced easily by changing the value of α^* in that segment. Of course, some matching conditions must be met to guarantee steady velocity distributions $V(x, \alpha)$ for every α over the total profile.

As will be shown, the multipoint design problems of hydrofoils require constant velocities in different segments of the profile for different angles of attack. The described method has been developed for direct solutions of such problems. Further discussions of this method are given in two recent papers by Eppler and Somers.[6,7] Comparisons of theory and experiments are given in Refs. 6, 10, and 11. For handling flap deflections, a potential flow analysis method is needed; thus, a higher order panel method has been developed and used in this analysis program. Details are described in Refs. 6 and 7.

A flap deflection is mathematically produced by rotating a part of the section around a flap hinge point; thus, a mathematical problem may occur near the hinge point. In practice, a concave corner will originate on one side, a convex, on the other. The radius decreases as the distance increases between the hinge point and the corresponding surface. In potential flow, a stagnation point forms at the concave corner, and a suction peak appears at the convex side near the flap hinge. In real flow, however, local boundary-layer separation occurring at the concave corner and boundary-layer displacement effects appearing at the convex arc smooth the flow. In the present potential flow treatment, both surfaces are smoothed near the flap hinge by circular arcs. An arc length of 3% chord width was found to give a good agreement between theoretical and experimental pressure distributions of a NACA 16-309 section.‡ This arc length will be used in the present studies.

Boundary-Layer Calculation

From the potential flow theory, the pressure distribution around an airfoil for every arbitrary angle of attack can be obtained. The pressure distribution, together with a Reynolds number Re based on the chord length, specify a boundary-layer flow around the airfoil. The boundary-layer calculation method uses a so-called one-parameter method based on the integral momentum and energy theorem,[5] which compute the momentum thickness θ, energy thickness δ^{**}, and shape parameter $H_{32} \equiv \delta^{**}/\theta$.

The boundary-layer calculation begins at the stagnation point with laminar flow. The boundary-layer transition from laminar to turbulent flow is determined by a simple semiempirical criterion based on the local Reynolds number:

$$R_{e_\theta} \equiv \frac{V}{V_\infty} \cdot \frac{\theta}{C} \cdot R_e$$

where V, V_∞, and C are local potential flow velocity, freestream velocity, and chord length, respectively. Transition is assumed to occur if [6,12,13]

$$R_{e_\theta} \geq R_{e_T} = 18.4 H_{32} - 21.74$$

The flow separation is assumed to occur if the shape parameter H_{32} is lower than 1.46 (see Refs. 6 and 7 for further discussions).

Design Objectives and Compromises

In designing a hydrofoil profile, compromises between different objectives must always be found. A hydrofoil craft should have a critical cavitation speed and a lift-to-drag ratio as high as possible. It is impossible to meet both objectives in one profile optimally. Thus, the first compromise used in this paper requires the constraint of no boundary-layer separation for all design conditions. Aside from this compromise, the following study will be considered with respect to extending critical cavitation speed.

Another constraint exists with respect to the thickness-to-chord ratio. It is known[4] that increasing τ allows less deep but wider pressure buckets in the minimum pressure envelope. In the present design, a thickness of at least $\tau = 0.09$ was assumed required, enabling good comparison to the NACA sections discussed previously. As it turned out, there was no reason for requiring a wider pressure bucket than could be obtained with $\tau = 0.09$; thus, this value was selected.

The next constraint concerns flap size. It has been shown that the pressure recovery has to start in front of the flap hinge; if not, a serious reduction of critical cavitation speed will occur with every flap deflection. Thus, a shorter flap

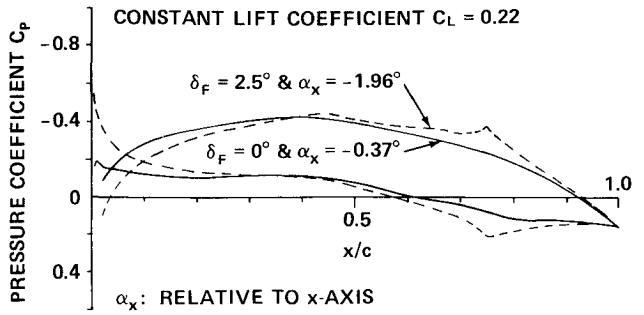

Fig. 4 Pressure distribution of NACA 64A309.

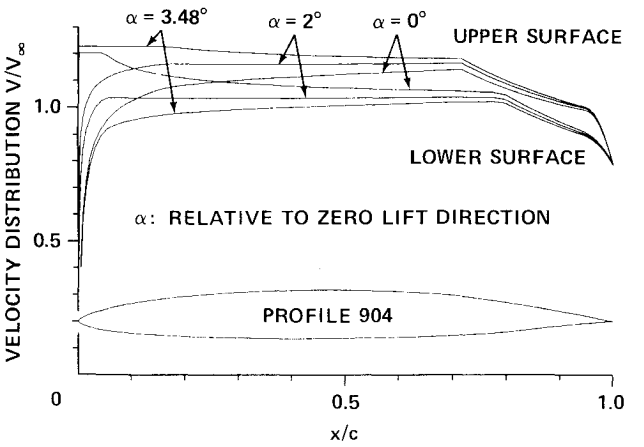

Fig. 5 Velocity distributions of Profile 904 at zero flap deflection.

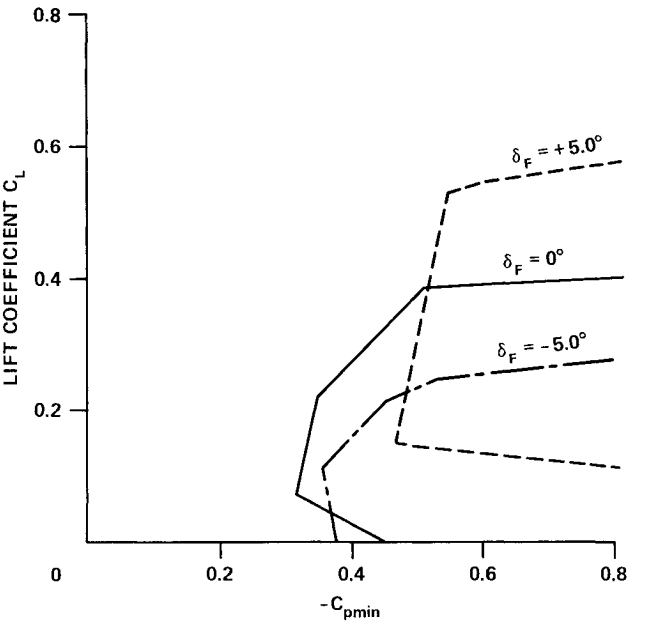

Fig. 6 Minimum pressure envelopes for Profile 904 at several flap settings.

chord allows later recovery and better $-C_{pmin}$, however, for structural reasons, the flap cannot be too thin. In the present designs, a flap chord of 20% of the main chord was considered adequate. This is reasonable compared to the 25% used for the NACA 64A 309 section, which is very thin near the trailing edge.

Finally, a compromise has to be found for the influence of sea conditions on the foil design. It was shown that a single-point like NACA 16-309 could be unfavorable even in a low sea state. The success of the design with respect to sea conditions can be evaluated by properties of the minimum pressure envelope in terms of either flap deflection δ_f or allowable change in angle of attack $\Delta\alpha$. A single-point design will be considered optimal if only one point of the envelope has a minimal $-C_{pmin}$. A better design could still be concentrated on one point, but would require that foil performance in the vicinity of this design point not be too degraded. Therefore, a pressure bucket must exist; however, the most important point is the center.

Another design could only be of interest for operation in high seas with some relaxation in the obtainable critical cavitation speed in a calm sea. This means two points would be considered; namely, the ends of the pressure bucket. All the design objectives give conditions for some corners in the pressure envelope. Every such corner occurs if the position of the minimal C_p changes abruptly. The corner corresponds to a pressure distribution which has C_p with either two different minima of the same absolute values or a segment of constant pressure. The second case always represents a partial optimum for $-C_{pmin}$. (Two isolated pressure minima can always be replaced by an area of constant pressure whose absolute value is higher than those of the two minima.) This is the reason why the described multipoint design method[5] allows direct optimization of some points in the pressure envelope by specifying segments with constant pressure. This procedure was applied to symmetrical profiles without flaps in Ref. 4. An extension of this approach to nonsymmetrical profiles without flaps is in preparation. The present paper tries to show also that the influence of flaps can be considered with little additional effort.

Two examples will be given. The first, Profile 904, is nearly a one-point design; the second, Profile 908, is a two-point design. Both sections met design conditions similar to the NACA 16-309 and NACA 64A309 ($a=0.8$) sections and will be compared to them. In these comparisons it is remarked that the nonsymmetrical NACA sections contain an approximation error, as the camber is introduced by a vortex distribution at the mean line. This inverse method[5] does not contain such a systematic error, and the algorithm admits minimal numerical errors.

High Critical Cavitation Speed with Regard to Low States of Sea (Profile 904)

The main objective in designing Profile 904 is to have a good value of $-C_{pmin}$ for the design point $C_L=0.22$ at the flap neutral position. The next objective is to have good flap effectiveness, at least within a certain range of flap deflections.

The solution to this design problem is given in Profile 904, as shown in Fig. 5, along with the most significant velocity distributions in the unflapped configuration. Velocity distributions for $\alpha=2$ deg at $C_L=0.22$ characterize the design point that meets the main objective. The upper surface velocity distribution is specified to have a constant velocity in the segment $0.15\leq x/c\leq 0.7$. By specifying $\alpha^*=2$ deg at that segment, a good value of $-C_{pmin}=0.35$ is realized at $C_L=0.22$. To prevent an early suction peak at the leading edge caused by the change in α or flap deflection, two more control points are introduced. At $\alpha=3.48$ deg, a constant velocity is introduced in the segment $0\leq x/c\leq 0.15$ of the upper surface with $\alpha^*=3.48$ deg. At $\alpha=0$ deg, a constant velocity is introduced in the segment $0\leq x/c\leq 0.05$ of the lower surface with $\alpha^*=0$ deg. These two control points prevent occurrence of a suction peak between $0\leq\alpha\leq 3.48$ deg. The corners of the pressure envelope which correspond to these control points can be seen in the solid line of Fig. 6. One additional corner corresponds to the foil angle α at which the occurrence of a minimum pressure point shifts from the upper to the lower surface or vice versa. This corner is at $C_L=0.07$ in Fig. 6. A long segment at the lower surface does not contribute to the shape of the pressure envelope. This segment

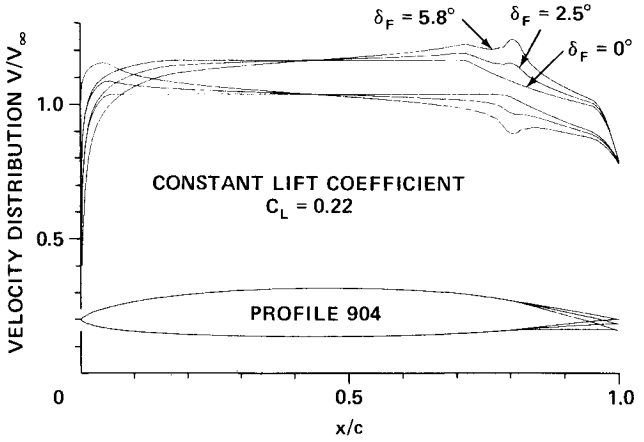

Fig. 7 Velocity distributions of Profile 904 at several flap settings.

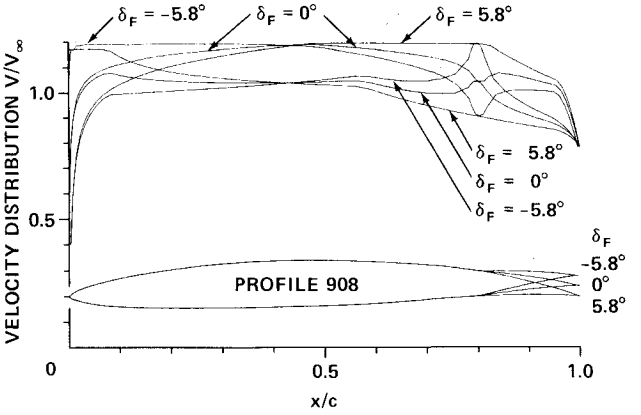

Fig. 9 Velocity distributions of Profile 908 at $\delta_F = -5.8$, 0, and 5.8 deg.

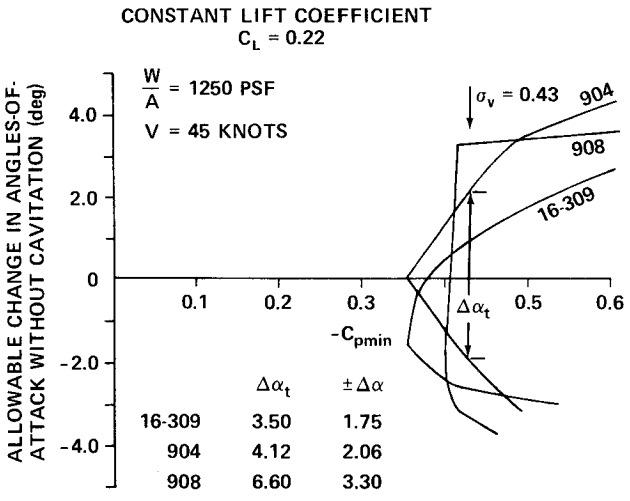

Fig. 8 Minimum pressure envelopes for Profiles 904, 908, and 16-309.

is introduced with $\alpha^* = 2$ deg, which gives a low enough velocity of the lower surface at hinge point.

The pressure recovery function used is concave. It has been shown by Wortmann[14] that the concave velocity distribution, apart from reducing the danger of boundary-layer separation, results in less drag than the velocity distributions of NACA wing sections. The nonseparated boundary layer would have admitted later recovery at the upper surface and, hence, a slightly lower value of $-C_{pmin}$. It will, however, accompany a sharp suction peak at the flap hinge line at flap down deflection. This will seriously restrict the capability of operating in sea states as observed in the NACA 16-309 section. To avoid this happening, pressure recovery on the upper surface is introduced earlier at $x/c = 0.7$. However, such a problem is not to be encountered at the lower surface owing to the positive design lift coefficient. Thus, the pressure recovery on the lower surface begins at $x/c = 0.8$. At the end of the trailing edge, a steep decrease in velocity (pressure recovery) on both sides of the profile is noticed on Fig. 5. This is the closure contribution, which is necessary for getting a reasonable trailing edge shape.

It now becomes important to discuss the flap-deflection cases. The question is, "What is gained in using this design approach with a sacrifice in having a higher value of $-C_{pmin}$ than will be necessary with the single-point design of an unflapped foil?" It has been assumed that the change in angles of attack on the foil due to waves is compensated by the difference in the zero lift angles due to flap deflection. The velocity distribution has to be shown for the same $C_L = 0.22$ at any flap deflection. This is done in Fig. 7 for $\delta_F = 2.5$ and 5.8 deg. Obviously, the suction peak at the lower side of the leading edge is not yet critical, and the suction peak at the hinge line is so reduced by the earlier recovery that it is responsible for $-C_{pmin}$ only if $\delta_F > 4.5$ deg.

The pressure envelope vs allowable change in angles of attack without cavitation is given in Fig. 8, where the flap efficiency of $\Delta\alpha/\delta_F = 0.55$ is used. This type of pressure envelope is similar to the pressure envelope plotted against the flap deflection δ_F. The only difference in these two envelopes is in the vertical scale. This type of pressure envelope is necessary in comparing profiles with different flap sizes. The corresponding pressure envelope for the NACA 16-309 section is also plotted in the same figure. The center of the pressure bucket for the NACA section is located at a negative flap angle of -1.7 deg. This offset may come from the nonexact design method. The pressure bucket of Profile 904 is seen to be wider than that of the NACA section, while the values of $-C_{pmin}$ are about the same for both profiles. However, it is noted that the good value of $-C_{pmin}$ achieved by the NACA 16-309 section involves a considerable penalty in section drag coefficient and early boundary-layer separation as this section has a convex pressure recovery function.

High Critical Cavitation Speed at High States of Sea (Profile 908)

To some degree, Profile 904 is an optimum section with respect to the compromise between a low value of $-C_{pmin}$ at the design point and the capability to tolerate a certain degree of fluctuation in angle of attack. However, the flapped cases give nonuniform velocity distributions on the foil. The sharp suction peak at the flap hinge line restricts its operable limit to a low sea state. Another objective for a profile design is to have as large as possible a range of flap-deflection angles at a constant value of $-C_{pmin}$. This corresponds to a one-speed design that will be operable at as high a sea state as possible. The minimum pressure envelope vs $\Delta\alpha$ for one lift coefficient must show a pressure bucket as wide as possible at a given depth. The solution of this problem is given by Profile 908 in Fig. 9.

Several facts are used in solving this problem.

1) At a constant C_L, a flap-down deflection causes an increase in velocity at the upper surface for $x/c > 0.45$ and a decrease in velocity for $x/c < 0.45$. At the lower surface, the trend is just the opposite. In addition, a flap-up deflection causes the velocity distributions to reverse the trend as do those in the flap-down case (see Fig. 7).

2) The flap-down deflection is limited by the occurrence of a suction peak at the flap hinge line of the upper surface and a leading edge suction at the lower surface.

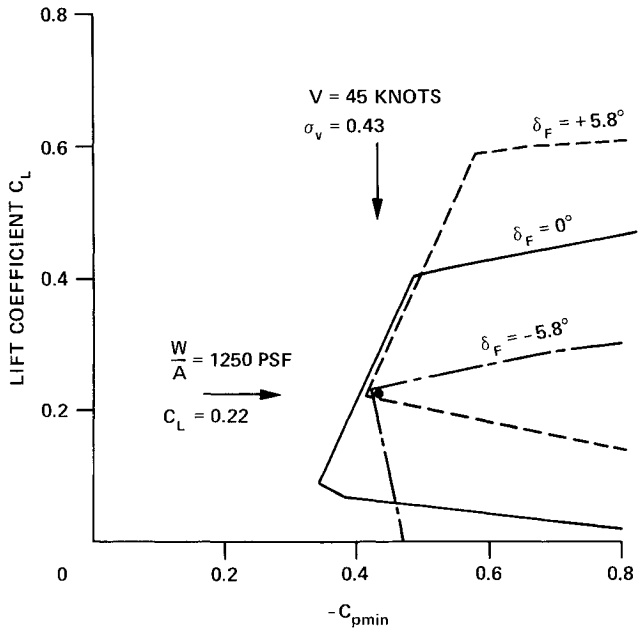

Fig. 10 Minimum pressure envelopes of Profile 908 at flap settings of −5.8, 0 and 5.8 deg.

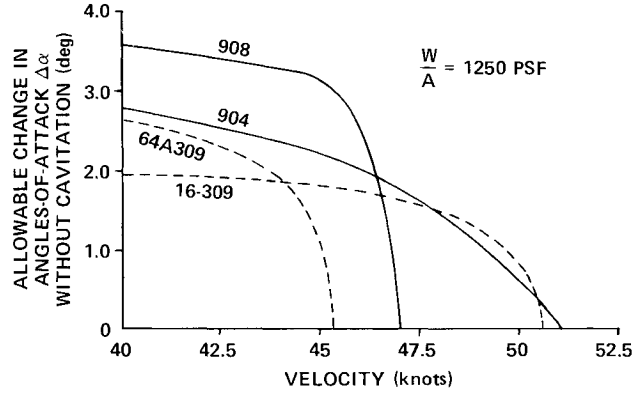

Fig. 11 Allowable change in angles of attack at incipient cavitation speeds for Profiles 904, 908, 16-309, and 64A309.

3) The case with flap-up deflection is limited by a suction peak at the flap hinge line of the lower surface and the leading edge suction at the upper surface.

The following approach yields a nearly optimum solution to the problem. A profile is designed for which only flap-up deflection is considered. The design is made in such a way that the flap-up deflection can be made as large as possible without penalizing $-C_{pmin}$. The pressure bucket against δ_F then ranges from $\delta_F = 0$ to $\delta_F = -\delta_{F\max}$, and there is no problem in defining the middle of the bucket $\delta_F = -1/2\delta_{F\max}$ as the unflapped case. It turns out that $\delta_{F\max} = 11.6$ deg is possible. In that sense, the design method is applied for the ±5.8-deg flap deflection. The critical segments are now on the upper surface behind $x/c = 0.45$ and on the lower surface near the leading edge. By introducing $\alpha^* = 2$ deg in both critical segments, this case is optimized. The length of the upper segment is limited by the allowable pressure recovery without separation at $Re = 3 \times 10^7$. The length of the lower segment has to be selected so that the velocities are about the same magnitudes in both segments.

About 90% of the lower surface length is specified in such a way that the hinge point has a low velocity, and no steep adverse pressure gradient is present. The velocity distribution of the upper surface front part at $0 \le x/c \le 0.45$ is manually iterated so that it becomes uniform in the flap-up case at $\delta_F = -5.8$ deg. This iteration is done by introducing many small segments and by iterating the corresponding α^* values. The procedure of varying α^* values in the flap-down case to produce the desired pressure gradient in the flap-up case can be easily done; see Ref. 5. The analysis program (direct method) is used to minimize the numbers of iteration needed.

Figure 9 gives the resulting profile and its most significant velocity distributions, while Fig. 10 gives the pressure envelopes vs the lift coefficient at three flap positions. At the lift coefficient $C_L = 0.22$ of the design, $-C_{pmin}$ occurs at $x/c = 0.45$ for all the flap settings. Additionally, it is noted that the same values of $-C_{pmin} = 0.42$ are obtained at $C_L = 0.22$ for all the flap settings between $-5.8 \le \delta_F \le +5.8$ deg. This results in an almost vertical line in the pressure bucket at Profile 908 at $-C_{pmin} = 0.42$ (see Fig. 8).

Profile 904 is based on a one-point design to minimize the value of $-C_{pmin}$ In a similar sense, development of the NACA 16 series was based on minimizing the value of $-C_{pmin}$ for application to high-speed propellers. Profile 908 is based on a two-point design to maximize the pressure bucket width at a given depth of pressure bucket. Similarly, the NACA 64 series was developed to maximize the laminar bucket width. The allowable changes in angle of attack without cavitation vs craft speeds at the foil loading of 1250 psf are shown in Fig. 11 for Profiles 908, 904, NACA 16-309, and NACA 64A309. Note the similarities in the shapes of operational envelopes for Profiles 904 and NACA 16-309 and Profiles 908 and NACA 64A309. Additionally, Fig. 11 shows the advantage of specifically developing profiles.

Conclusion

This study has shown the development of a suitable foil section depends on the operational requirements of each hydrofoil craft. Two examples given in this study have shown that it is possible to design hydrofoil sections having improved critical cavitation speed with and without flap deflection and simultaneously improved boundary-layer behavior. Experimental verification should be followed. We are far from propagating these examples for common application; however, we are convinced that refining a profile for every special application will be possible and advantageous in the future.

Acknowledgments

Grateful appreciation is expressed to D. Cieslowski for this helpful discussion and R. Wermter for his encouragement. The work carried out by one of the authors was supported under Naval Material Command 08T, Program Element 62543N, Subproject ZA 43-421-001.

References

[1] Ellsworth, W.M., "U.S. Navy Hydrofoil Craft," *Journal of Hydronautics*, Vol. 1, 1967, pp. 66-73.

[2] Abbott, I.H. and von Doenhoff, A.E., *Theory of Wing Sections*, Dover Publications, New York, 1959.

[3] Layne, D.E., "Lift and Drag Characteristics of NACA 16-309 and NACA 64A309 Hydrofoils," David W. Taylor Naval Ship Research and Development Center Report SPD-326-07, Oct. 1976.

[4] Eppler, R. and Shen, Y.T., "Wing Sections for Hydrofoils," to be published in the *Journal of Ship Research*.

[5] Eppler, R., "Direkte Berechnung von Tragflügelprofilenen aus der Druckverteilung," *Ingeneiur-Archiv*, Vol. 25, 1957, pp. 32-59.

[6] Eppler, R. and Somers, D.M., "Low Speed Airfoil Design and Analysis," Advanced Technology Airfoil Research Conference, Langley Research Center, NASA, Hampton, Va., March 1978.

[7] Eppler, R. and Somers, D.M., "A Computer Program for the Design and Analysis of Low Speed Airfoils," NASA Tech. Memo. (to be published).

[8]Shen, Y.T. and Peterson, R., "Unsteady Cavitation on an Oscillating Hydrofoil," Twelfth Symposium on Naval Hydrodynamics, Washington, D.C. June 1978.

[9]Feifel, W.M., "Design and Evaluation of Two Hydrodynamically and Structurally Optimized Foil Sections," Boeing Company, Boeing Marine Systems, Rept. D321-51507-2, July 1977.

[10]Miley, S.J., "An Analysis of the Design of Airfoil Sections for Low Reynolds Numbers," Mississippi State University, Ph.D. Thesis, 1972.

[11]Freuler, R.J. et al., "An Evaluation of Four Single-Element Airfoil Analytic Methods," Advanced Tehnology Airfoil Research Conference, Langley Research Center, NASA, Hampton, Va., March 1978.

[12]Eppler, R., "Praktische Berechnung laminarer und turbulenter Absauge-Grenzschichten," *Ingeneiur-Archiv.*, Vol. 32, 1963, pp. 221-245.

[13]Eppler, R., "Laminarprofile für Reynolds—Zahlen grösser als 4 $\times 10^6$," *Ingeneiur-Archiv.*, Vol. 38, 1969, pp. 232-240.

[14]Wortmann, F.S., "Progress in the Design of Low Drag Aerofoils," *Boundary Layer and Flow Control*, Vol. 2, G.V. Lachmann (Ed.), Pergamon Press, London, 1971, pp. 548-770.